NRL Memorandum Report 4486

Catalyzed Combustion of Carbon Fibers From Carbon Fiber-Resin Composites

J. GANJEI, D. DOMINGUEZ, J. MACKEY, AND J. MURDAY

Surface Chemistry Branch
Chemistry Division

April 22, 1981

NAVAL RESEARCH LABORATORY
Washington, D.C.

SECURITY CLASSIFICATION OF THIS PAGE (When Data Entered)

REPORT DOCUMENTATION PAGE		READ INSTRUCTIONS BEFORE COMPLETING FORM
1. REPORT NUMBER NRL Memorandum Report 4486	2. GOVT ACCESSION NO. AD-A098	3. RECIPIENT'S CATALOG NUMBER 046
4. TITLE (and Subtitle) CATALYZED COMBUSTION OF CARBON FIBERS FROM CARBON FIBER-RESIN COMPOSITES		5. TYPE OF REPORT & PERIOD COVERED Final Report 10/77–10/80 6. PERFORMING ORG. REPORT NUMBER
7. AUTHOR(s) J. Ganjei, D. Dominguez, J. Mackey*, and J. Murday		8. CONTRACT OR GRANT NUMBER(s)
9. PERFORMING ORGANIZATION NAME AND ADDRESS Naval Research Laboratory Washington, DC 20375		10. PROGRAM ELEMENT, PROJECT, TASK AREA & WORK UNIT NUMBERS 62761N; WF61542001; 61-0093-0-1
11. CONTROLLING OFFICE NAME AND ADDRESS Naval Air Systems Command Washington, DC 20361		12. REPORT DATE April 22, 1981 13. NUMBER OF PAGES 75
14. MONITORING AGENCY NAME & ADDRESS(if different from Controlling Office)		15. SECURITY CLASS. (of this report) UNCLASSIFIED 15a. DECLASSIFICATION/DOWNGRADING SCHEDULE

16. DISTRIBUTION STATEMENT (of this Report)

Approved for public release; distribution unlimited.

17. DISTRIBUTION STATEMENT (of the abstract entered in Block 20, if different from Report)

18. SUPPLEMENTARY NOTES

*Participant in NSF-sponsored American University summer research program for high school students.

19. KEY WORDS (Continue on reverse side if necessary and identify by block number)

Carbon fiber
Graphite fiber
Catalyst
Combustion
Graphite/Epoxy
Composites
Carbon oxidation

20. ABSTRACT (Continue on reverse side if necessary and identify by block number)

A Government-wide program was developed in response to the potential electrical hazards associated with carbon fiber release from carbon fiber composites used as structural materials for military aircraft. Fibers can be released during/after accidental burn or burn/blast scenarios where the composite epoxy ignites and is burnt off, leaving the base carbon fiber structure behind. Under these conditions, the major process for fiber gasification is the reaction of carbon and oxygen to form carbon monoxide and carbon dioxide. The rate of fiber oxidation can be enhanced considerably by the addition of metal

(Continues)

DD FORM 1 JAN 73 1473 EDITION OF 1 NOV 65 IS OBSOLETE
S/N 0102-014-6601

SECURITY CLASSIFICATION OF THIS PAGE (When Data Entered)

20. ABSTRACT (Continued)

catalysts to the fiber surface when the rate is not controlled by reactant oxygen diffusion. The work performed by the Chemistry Division of the Naval Research Laboratory involved the implementation and evaluation of metal additives to the composite epoxy resin for enhancing the gasification of carbon fibers, thereby reducing the amount of fibers left for release.

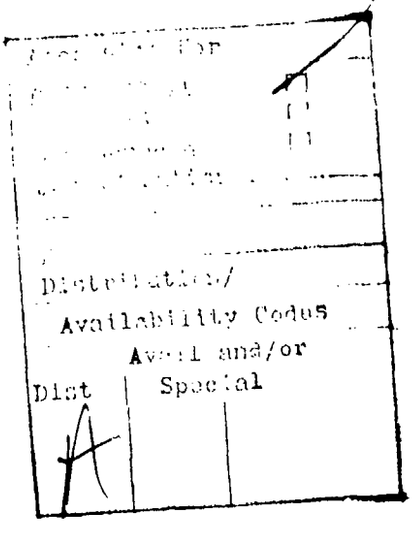

CONTENTS

EXECUTIVE SUMMARY

A Government-wide program was developed in response to the potential electrical hazards associated with carbon fiber release from carbon fiber composites used as structural materials for military aircraft. Fibers can be released during/after accidental burn or burn/blast scenarios where the composite epoxy ignites and is burnt off, leaving the base carbon fiber structure behind. Under these conditions, the major process for fiber gasification is the reaction of carbon and oxygen to form carbon monoxide and carbon dioxide. The rate of fiber oxidation can be enhanced considerably by the addition of metal catalysts to the fiber surface when the rate is not controlled by reactant oxygen diffusion. The work performed by the Chemistry Division of the Naval Research Laboratory involved the implementation and evaluation of metal additives to the composite epoxy resin for enhancing the gasification of carbon fibers, thereby reducing the amount of fibers left for release.

The results of the NRL work can be summarized by the following points:

1. The effect of metal additives was observed in increasing the gasification rate in a fuel fire and the amount of self-sustained combustion after removal from the fire. In general, gasification rates within the reducing environment of the fire were very slow and relative rates were proportional to oxygen accessibility as well as the presence of metal additives. As a result, self-sustained combustion is considered a major factor for fiber gasification.

2. In all tests the most effective additive was Pb in the form of acetates or oxides. A concentration of .01 g atom Pb/100 g epoxy (which resulted in Pb/C surface atomic ratios >1 %) was a minimum amount for effective catalysis with multiply composites. Preliminary results indicate that this did not affect the composite mechanical properties. The ranking of the next effective catalysts was Bi > V > Cu > Li, Cs, K. Most other metal additives exhibited equivalent activity, which was higher than untreated composites.

3. The amount of self-sustained combustion weight loss depended on the heat balance between the exothermic oxidation reaction and the heat loss. This balance was successfully modeled and the model explained the effects of metal catalysts and experimental features.

4. The Pb additive resulted in >90% fiber wt. loss for ≥4 ply composites and ≈ 40-50% wt loss for 4 ply fabrics and single tows during self-sustained combustion. This was observed for Epon 828 epoxy composites at room temperature, atmospheric air and natural convection after 1-minute exposure to fuel fires. Composites with 3501-6 epoxy and Pb additives needed either a fuel fire exposure time >2 mins, high Pb_3O_4 epoxy concentration (.1 g atom/100 g), or high ambient flow velocities to reproduce the >90% wt. loss. The 3501-6 inhibiting effect may be due to sulfur residue left on the fiber surface.

In terms of accident scenarios, we make the following predictions. The metal additive can substantially reduce fiber release from the fabric structure during/after a fuel fire. The most dramatic effect of the catalysts is to sustain fabric and tow combustion within a natural atmosphere, room temperature environment after removal from the fire. If a single fiber has been released into the air from the fabric, its high convective heat loss will extinguish the catalyzed oxidation reaction. Blast velocity release might also extinguish combustion of fiber/composite aggregate due to the high convection heat loss.

CATALYZED COMBUSTION OF CARBON FIBERS FROM CARBON FIBER-RESIN COMPOSITES

I. INTRODUCTION

This report describes the work performed by Code 6170 of the Naval Research Laboratory in support of the program of materials modification of carbon fiber composites. This program was initiated in response to the potential electrical hazard associated with carbon fiber release during accidental fires. The problem was deemed especially serious by the Navy due to the percentage of carbon fiber composites in the structural components of the Navy F-18 combat aircraft and the high projected usage in future combat aircraft. Recently, detailed risk analyses have been carried out for possible accident scenarios involving both commercial and military products containing carbon fiber composites. These analyses have concluded that the present and short-term future economic and military consequences of carbon fiber release are minimal. The commercial risk analysis is available as NASA Conference Publication 2119; the proceedings of the December 4-5, 1979, briefing at NASA Langley Research Center, Hampton, VA. The military risk analysis was summarized in the June 5, 1980, Havename meeting at NSWC, Silver Spring, Md.

The NRL work focused on reducing the electrical hazards caused by fiber release by promoting fiber combustion during/after an accidental fire. The selected method was the addition of metal promoters to the composite epoxy which would increase the reaction rate of $C + O_2 \rightarrow CO + CO_2$, thereby converting fibers into gaseous products. This solution is potentially simple to implement since

Manuscript submitted February 5, 1981.

it only involves mixing the epoxy with a small amount of powder additive. Ideally, the additive would remain an inert material until released by the accidental fire/explosion scenario. Two other solutions, epoxy modification to produce charring for increased fiber retention, and fiber modification to reduce conductivity, are inherently long-range solutions because they would require more extensive materials requalification.

The experimental program developed into several distinct phases: choice of metal compound as combustion promoters, method of addition to the composite, and effect of experimental conditions on oxidative rates. Based on this experimental work and on combustion theory, a model for fiber combustion is developed which identifies the important features of oxidation with and without metal additives. The effects of air flow, sample geometry, ambient temperature, and combustion promoters are incorporated into this model. The roles of reaction kinetics, radiative heat loss, and sample surface temperature are discussed in detail. Two other laboratories, Jet Propulsion Laboratory and NADC in Warminster, PA., performed work in this area, and their results will be mentioned at appropriate places.

In the Conclusion we will discuss the viability of combustion promoter additives to increase carbon fiber gasification.

II. EXPERIMENTAL TESTING

A. Selection of Oxidation Promoter

The carbon literature contains a large number of publications concerning the oxidation of different forms of carbon by oxygen. At least fifty years ago it was noted that the oxidation reaction rate could be increased by the presence of metal impurities on the surface of the carbon. Since then, many papers have reported this phenomenon in terms of reaction rates with different metal additives.

As a result, most work on selection catalyst at NRL was performed on an empirical basis. "Good" catalysts from the literature were introduced to the specific carbon fiber system of interest. Several criteria were used to evaluate the metal catalysts. The first test was the spontaneous ignition temperature (SIT) of the fibers treated with a 0.1M solution of the metal salt in water. The second test measured the amount of weight loss in the self-sustained combustion (combustion at room temperature environment) mode after fiber ignition within a heat source. The third test measured fiber weight loss in self-sustained combustion from a composite impregnated with the metal additive. The third test was the most critical, since the fiber composite is the actual structural material of interest to the Navy. The first two tests, however, were easier to perform since composite preparation is a more time-consuming process. In addition, the bare fiber tests provided a baseline measurement to compare with different composite geometries and epoxy mixtures.

1. Spontaneous Ignition Temperature (SIT)

The SIT test has been extensively used in the literature to measure the relative activity of oxidation promoters. (2) Since the $C + O_2$ reaction is exothermic, releasing between 25 to 80 kcal/mole depending on whether CO or CO_2 is the major product, ignition routinely occurs in carbon oxidation. Spontaneous ignition is defined as the temperature at which reaction produces a thermal runaway and the carbon surface temperature becomes significantly higher than ambient. The rationale behind the SIT test is that the lower the SIT, the more effective the promoter is in increasing the carbon oxidation rate. The test assumes that ignition always occurs at approximately the same oxidation rate. This assumption is only valid if the experimental conditions and sample matrix are reproduced in each measurement. The disadvantage of the SIT test is that it does not directly measure the effect of the additive on sustaining combustion after ignition in a fuel fire scenario.

The SIT measurements were accomplished on a Dupont 990 Thermal Analyzer in the thermal gravimetric analysis (TGA) mode at 250 ml/minute air flow and a heating rate of 20°C/min. A typical TGA plot is shown in Figure 1. The ignition point is shown as a sharp decrease in weight and a discontinuous jump in temperature due to the reaction exothermicity. Sample preparation was accomplished by dipping the fibers in 0.1M aqueous solution of the metal salt, drying the fibers on filter paper at ambient temperature and subsequently, a drying oven at 100°C. This preparation should result in equivalent surface concentration of the various metals on the fibers since we assume a physical adsorption mechanism. Most

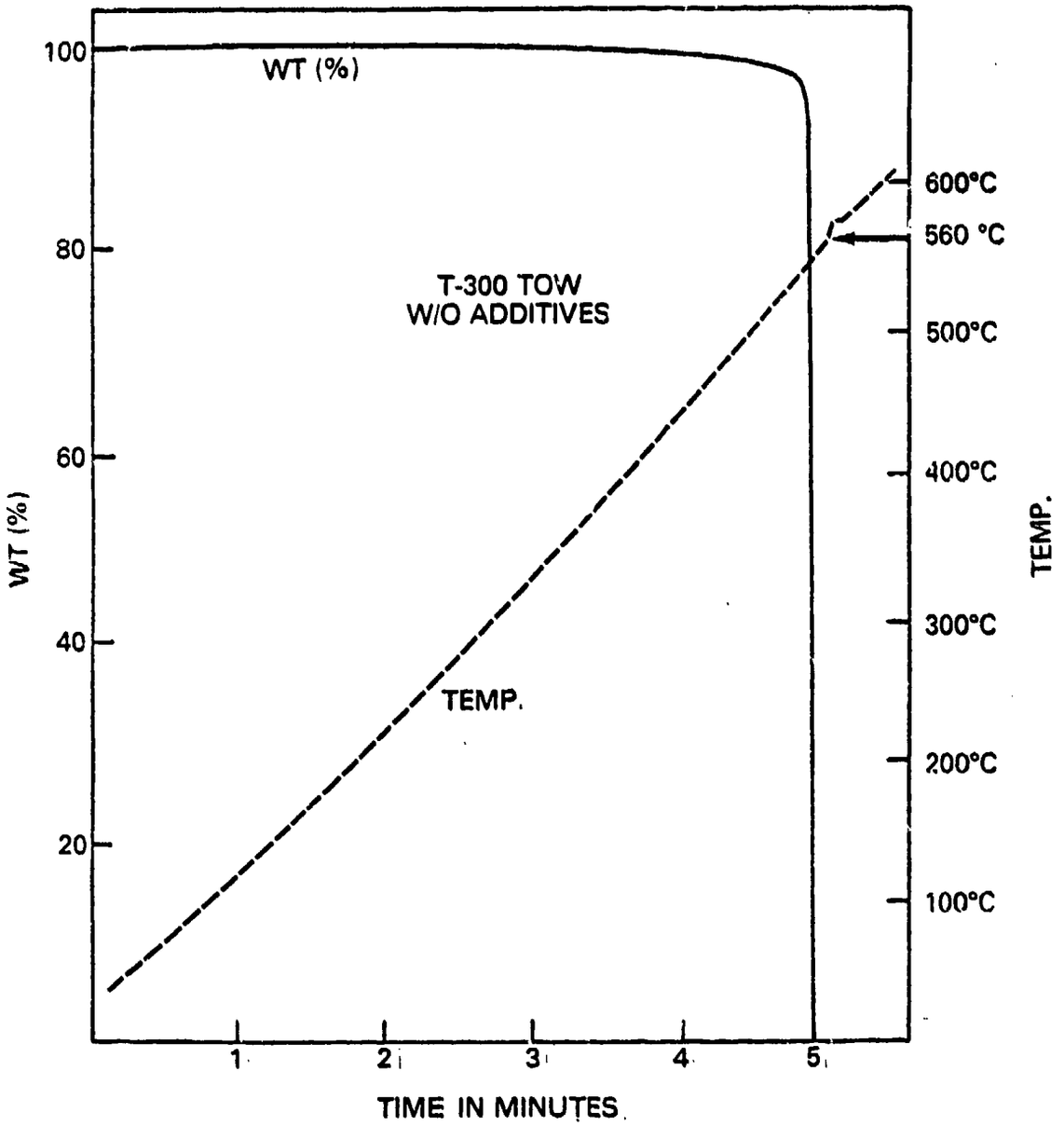

Fig. 1 — TGA of virgin T-300 tow at 20°C/min heating rate and 250 ml/min air flow

metals were added as acetates. However, acetates were unavailable for all the metals and other salts were also used. In some cases, nitric acid was added to increase the solubility of the non-acetate salts in water.

The results in Table 1 show that Pb was the most effective metal in lowering the SIT for tows of Thornel 300 carbon fibers. The temperature difference between the Pb-treated and the control tows was approximately 200°C. (The control SIT is believed to be 550°C and the lower SIT values are due to contamination.) Bismuth salts were a close second. The next rank at ~120°C difference include Li, V, Cs, and perhaps K. Other metal treatments lowered the SIT by 50-70°C. The same hierarchy was observed for Hercules AS tow analyses, but the SIT's were consistently 30-40°C higher. The 30-40°C gap probably reflects the fact that the AS fiber has a lower surface area than the T-300 fiber. The sensitivity of this test to the experimental conditions such as metal concentration, fiber type, and air flow was shown by other data not presented here in which the SIT measurements changed significantly upon variation of the above parameters.

Similar weight loss vs temperature curves were produced for composites of T300 fabric (composite preparation described in Appendix A) and the results are presented in Table 2. In this case, the initial weight loss represents epoxy weight loss (epoxy did not ignite at 20°C/min heating rate) and the fiber ignition occurs after epoxy loss. All the additives reduced the composite fiber SIT by 70°C at the three different air flows. The untreated

Table 1 — Spontaneous ignition temperature (SIT) of single fiber T-300 tows at 250 ml/min air flow and 20°C/min. Heating rate

.1M Metal Acetate Solution	SIT (°C)
Pb	340, 350, 350, 360
Pb/Li	370
$Pb(NO_3)_2$	370
$Bi(NO_3)_3$	380
V	425
Cs	430
Li	430, 440
K	440, 450, 470
Na	450, 460, 480
Ba	470, 475
Ca	485, 480, 485
Sr	485
Cu	480, 500, 510
$AqNO_3$	500
Control	470, 485, 540, 560
Co	520
Cr	540
Mn	550
Ce	580

Table 2 — SIT temperatures of composites[a]

Fiber-Epoxy	Ply	Additive	50% Epoxy Wt. Loss	SIT	Oxidation Rate After SIT	O_2 Flow Rate
T-300 Epon 828	6	Bi_2O_3	415°C	510°C	5%/min.	50 ml/min.
T-300 Epon 828	6	-	410°C	580°C	6%/min.	50 ml/min.
T-300 Epon 828	6	$Ca(OAc)_2$	410°C	510°C	5%/min.	50 ml/min.
T-300 Epon 828	6	PbO	410°C	500°C	5%/min.	50 ml/min.
T-300 Epon 828	6	CuO	410°C	500°C	6%/min.	50 ml/min.
T-300 Epon 828	6	Pb_3O_4	405°C	500°C	6%/min.	50 ml/min.
T-300 Epon 828	6	Pb_3O_4	400°C	485°C	11%/min.	150 ml/min.
T-300 Epon 828	6	-	405°C	580°C	1%, 11%	150 ml/min.
T-300 Epon 828	6	Pb_3O_4	390°C	475°C	18%/min.	250 ml/min.
T-300 Epon 828	6	-	400°C	545°C	1%, 3%	250 ml/min.

[a]Samples described in Table 5.

composites also showed an induction period of slow oxidation after epoxy decomposition. The epoxy reactions as measured by the 50% wt loss temperature were not affected by the metal additives.

2. Fabric Self-Sustained Combustion

The second test consisted of igniting single-ply fabric in a 700°C furnace, removing the fabric from the furnace and measuring the weight loss during self-sustained combustion. In practice, it was extremely difficult to separate fabric self-sustained weight loss from weight loss within the furnace. As a result, total weight loss was measured and the control weight loss subtracted from treated fabric weight loss. In addition, total burn time outside the furnace was also estimated. These results are presented in Table 3 for T-300 fabrics and Table 4 for AS fabrics. The only significantly different weight loss enhancement was achieved by Pb compounds in both fabrics and Bi in the T-300 fabrics. When the cloth was treated with two metals, the recorded weight loss was equivalent to the more effective metal additive by itself, and no synergistic effect was discernible. The untreated AS fabric also showed significantly less weight loss (11% compared to 24%) than the T-300 control. These results correlate with the observation that propagation of combustion in a tow when lit at one end was only obtained with Pb-treated T-300 fibers. However, the maximum weight loss exhibited by Pb-treated single tows or single-ply fabric was consistently found to be ≈50%.

Table 3 — Self-sustained combustion of T-300 fabric

Solution .1M	% Wt. Loss	% Wt. Loss Minus Control % Wt. Loss	Burn Time Out of Oven
$Pb(OAc)_2$	67 56	43 32	.6 .9 mins.
$Pb(OAc)_2 + Na_2CO_3$ [6,7]	58 48	34 24	.8 .6
$Pb(OAc)_2 + Ca(OAc)_2$ [6]	51	27	.7
$Bi_2O_2CO_3$ [1]	42	18	.8
Ag_2CO_3 [1]	39	15	.3
$Ca(NO_3)_2$	39	15	.4
LiOAc	37	13	.2
Cs_2CO_3 [1]	36 35	12 11	.1 .3
$Ca(OAc)_2$	36	12	.3
$Ba(OAc)_2$	36	12	.3
$Ca(NO_3)_2 + Na_2CO_3$ [1,6]	35	11	.2
$NaOAc + Ca(OAc)_2$ [6]	35	11	.2
$Cu(OAc)_2$	35	11	.2
$Sr(NO_3)_2$	35	11	.4
$Ca(OAc)_2$ [5]	35	11	.2
$Mn(OAc)_2$	36 33	9 12	.3 .4
$Co(OAc)_2$	34	10	.4
Na_2CO_3	33 31	9 7	.1 .1
NaOAc	31	7	.1
KOAc	31	7	.1
$Ce(NO_3)_3$	35 15	11 -9	.2 .3
$Cr(OAc)_3$	26	2	.1

Table 3 (Cont'd) — Self-sustained combustion of T-300 fabric

Solution .1M	% Wt. Loss	% Wt. Loss Minus Control % Wt. Loss	Burn Time Out of Oven
$V(OAc)_4$ [1,2,3]	24	0	.1 mins.
$Mg(OAc)_2$	30 18	6 -6	.2 .2
Control	24	0	.1
$Fe(OAc)_3$ [1,2,3,4]	23	-1	.1
$Zn(OAc)_2$	22 13	-2 -11	.2 .1

[1] Concentrated HNO_3 added

[2] May be poor solution

[3] Saturated solution

[4] ppt

[5] .2M solution

[6] .1M of each

[7] Cloudy

Table 4 — Self-sustained combustion of AS fabric

Solution	% Wt. Loss	% Wt. Loss Minus Control % Wt. Loss	Burn Time Out of Oven (min.)
Pb + Bi(OAc)	39	28	.5
$Pb(OAc)_2$	38	27	.55
$Bi_2O_2CO_3$	36	25	.45
Pb + Ca (OAc)	35	24	.4
Pb + Li (OAc)	34	23	.4
Bi + Na (OAc)	33	23	.3
LiOAc	31	20	.25
$Co(OAc)_2$	30	19	.25
Aq_2CO_3	30	19	.2
$Mn(OAc)_2$	30	19	.2
$Ba(OAc)_2$	29	18	1.3
$Cu(OAc)_2$	29	18	.25
Cs_2CO_3	29	18	.25
$Sr(NO_3)_2$	28	17	.2
NaOAc	28	17	.1
$Ca(OAc_2)$	27	16	.2
$V(OAc)_4$	27	16	.1
K(OAc)	27	16	1.1
$Ce(NO_3)_3$	26	15	.1
$Fe(OAc)_3$	24	13	.15
$Cr(OAc)_3$	18	7	.1
$Zn(OAc)_2$	12	1	.1
$Mg(OAc)_2$	11	0	1.1
Control	11	-	.1

3. Composite Self-Sustained Combustion

This third test has been previously described in an NRL report (3). Composite preparation is described in detail in Appendix A. The fabric was laid up with epoxy and/or additives to about 30% by weight of epoxy. Curing and lay-up procedure were not carefully controlled except for the mechanical test samples. Additive weight percentage was measured to approximately .01 g atoms/100 g. resin. The different samples are listed in Table 5. The combustion test was performed by igniting the epoxy in a 600-700°C oven, removing the fabric after the epoxy flame has self-extinguished, and measuring the self-sustained combustion weight loss. As discussed in the previous report, air flow had a large effect on combustion, and our results were obtained with the chamber door open. After fiber ignition, visually observed by sample glowing red at higher temperature than oven temperature, further time in the oven had no effect on the self-sustained weight loss. The weight loss results are listed in Table 6 for T-300 fabric in Epon 828, Table 7 for AS fabric in Epon 828, and Table 8 for AS fiber in 3501-6 epoxy.

The results in Table 6 show the T-300 Epon 828 composite system loses all the epoxy in the first minute and fiber combustion has begun in the oven. Upon sample removal from the oven, the Cu, Bi, and Pb-treated samples continue combustion; the most complete combustion is achieved by the Pb samples. The weight loss percentage is similar for both the 6- and 24-ply samples and is substantially greater than the single-ply fabric weight losses. However, the weight loss rate for the composite was inversely

Table 5 — Sample composites prepared for study

Fiber	Epoxy	Additive	Wt. % Epoxy	g atom /100 g resin	Sample	Ply
T-300	Epon 828	-	33	-	N 5728-69	4
T-300	Epon 828	-	33	-	5728-81	6
T-300	Epon 828	CuO	36.2	.01	5728-82	6
T-300	Epon 828	$CaCO_3$	35.7	.01	5728-83	6
T-300	Epon 828	PbO	34.9	.01	5728-84	6
T-300	Epon 828	Pb_3O_4	35.8	.01	5728-86	6
T-300	Epon 828	$Ca(OAc)_2H_2O$	38.8	.01	-87	6
T-300	Epon 828	$Bi_2O_2CO_3$	33.8	.01	FL-2	6
T-300	Epon 828	Bi_2O_3	38.5	.01	FL-3	6
T-300	Epon 828	-	32.2	-	FL-13	6
T-300	Epon 828	$CaCO_3$	33	.01	FL-14	6
T-300	Epon 828	CuO	34.0	.01	FL-15	6
T-300	Epon 828	Pb_3O_4	35.8	.01	FL-16	24
T-300	Epon 828	-	34.4	-	FL-17	24
T-300	Epon 828	Sb_2O_3	33.8	.01	FL1-47	6
As	Epon 828	PbO	30.6	.01	FL-7	4
As	Epon 828	Pb_3O_4	31.5	.01	FL-8	4

Table 5 (Cont'd) — Sample composites prepared for study

Fiber	Epoxy	Additive	Wt. % Epoxy	g atom /100 g resin	Sample	Ply
As	Epon 828	Pb_3O_4	30.3	.002	FL-9	4
As	Epon 828	CuO	32.3	.01	FL-6	4
As	Epon 828	$CaCO_3$	41.1	.01	FL-5	4
As	Epon 828	Pb_3O_4	31	.005	FL-12	4
As	Epon 828	-	34.5	-	FL-4	4
Gy-70	Epon 828	-	34.7	-	FL-10	8
Gy-70	Epon 828	Pb_3O_4	40.3	-	FL-11	8
As prepreg	3501-6	$CuCO_3$	29.2	.01	FL-21	12
As prepreg	3501-6	CuO	29.3	.01	FL-20	12
As prepreg	3501-6	Pb_3O_4	29	.01	FL-19	12
As prepreg	3501-6	-	28.2	-	FL-18	12
As fabr.	3501-6	Bi_2O_3	31.5	.01	FL-30	4
As fabr.	3501-6	-	31.8	-	FL-31	4
As fabr.	3501-6	Pb_3O_4	33.8	.01	FL-32	4
As fabr.	3501-6	Pb_3O_4	-	.1	FL-33	4

Table 6 — Self-sustained combustion of T-300 composites after oven ignition for 1 min.

Metal Cmpd.	Epoxy	Fabric Ply	Total Wt. Loss %	Fiber Wt. Loss %	Burn Time Out of Oven in Min.
[illegible]O	Epon 828	6	97	95	7.6
Pb_3O_4	Epon 828	6	96	93	5.2
Bi_2O_3	Epon 828	6	92	87	5.7
CuO	Epon 828	6	76	64	5.5
$Ca(OAc)_2H_2O$	Epon 828	6	61	37	-
	Epon 828	-	52	22	2.6
Control	Epon 828	6	50	26	1.8
Sb_2O_3	Epon 828	6	45	17	1.3
Pb_3O_4	Epon 828	24	98	97	22.0
	Epon 828	-	97	96	-
Control	Epon 828	6	42	9	2.5
	Epon 828	-	40	8	2.3

Table 7 — Self-sustained combustion of AS composites after oven ignition for 1 min.

Metal Cmpd.	Epoxy	Fabric Ply	Total % Wt. Loss	Fiber % Wt. Loss	Burn Time Out of Oven in Mins.
PbO	Epon 828	4	94.8	87	8.0
Pb_3O_4 (.610)	Epon 828	4	73.6	61	5.6
Pb_3O_4 (.305)	Epon 828	4	56.8	35.8	.85
$CaCO_3$	Epon 828	4	48.2	20.9	.45
Pb_3O_4 (.122)	Epon 828	4	43.0	15	.8
CuO	Epon 828	4	42.3	15	.45
Control	Epon 828	4	44.3	13.4	.35
Pb_3O_4	Epon 828	12	94.8	92.9	15.0
CuO	Epon 828	12	35.4	7.1	.7
Control	Epon 828	12	35.1	7.1	.7
$CaCO_3$	Epon 828	12	34	7.0	.5

related to number of plys in the composite. During the tests, we observed that expansion of the distance between the fabric plys due to turbulence resulted in extinguishing combustion of the outside layers. If fanning out was extreme, the inside layers also extinguished. The longest combustion time was always achieved by the inside layers. We will explain these observations in the model section by postulating that radiative heat loss is the major cause of extinguishing and outside layer reaction prevents the oxygen reactant from reaching the inside layers. Inside layers continue combustion since their heat loss is diminished by radiative adsorption from hot surrounding layers but their oxidation rate is slower. The single-ply fabric experiences minimal self-adsorption and therefore has the greatest heat loss/unit area, which results in the lowest self-sustained combustion weight loss.

Table 7 lists the AS Epon 828 composite data. In this system, the control weight loss is only ≈13%, as compared to 25% for the T-300 Epon 828 results. The Cu-treated AS Epon/828 has approximately the same weight loss as the control, whereas Cu-treated T-300 lost over 50% original fiber weight. Even the Pb_3O_4-treated six-ply samples do not achieve the same weight loss as found for Pb_3O_4-treated T-300/Epon 828. Only the PbO six-ply and Pb_3O_4 12-ply lost over 90% original fiber weight. The effect of concentration is shown in the .610 g Pb_3O_4 (.01 g-atoms Pb/100 g resin), .305 g (.005 g-atoms Pb/100 g resin), and .123 g Pb_3O_4 (.002 g-atoms Pb/100 g resin) samples where the decreasing metal concentration results in decreasing fiber weight loss. On the basis of this test and others, the minimum effective Pb_3O_4 concentration was determined to be .01 g-atoms/100 g resin.

The results of the last system, AS fiber in 3501-6 epoxy, are shown in Table 8. The burn times out of the oven are extremely short for all the samples and so, as a result, the self-sustained combustion weight losses are below 10%. Since the metals were effective in promoting oxidation with the AS fiber-Epon 828 system, we immediately suspected that the inhibiting effect was due to the 3501-6 epoxy. A similar composite with 10X Pb_3O_4 concentration was also made up and its performance is listed in the last row of Table 8. The increase in Pb_3O_4 concentration was able to overcome the 3501-6 epoxy effect. However, this composite had a prohibitively high amount of additive (6.85 g Pb_3O_4 per 100 g epoxy).

B. Microscopy of Fibers

This section describes the morphology and elemental composition of carbon fiber surfaces after various treatments. The data were obtained by the use of scanning electron microscopy (SEM) with energy dispersive x-ray analysis (EDAX), Auger electron spectroscopy (AES) and x-ray photoelectron spectroscopy (XPS, also known as electron spectroscopy for chemical analysis, ESCA). We examined virgin fibers and composite fibers after the epoxy had been burnt off. The composite analysis was limited to samples which contained Pb additives since our main interest was oxidative attack promoted by Pb. We also carefully examined the 3501-6 composite fibers, since the 3501-6 epoxy residue had an inhibiting effect on fiber oxidation.

Table 8 — Self-sustained combustion of AS fiber 3501-6 epoxy from oven ignition

Composite	Temp. (°C) of Oven	Time In Oven (Mins)	Burn Time Out of Oven (Min)	Total % Wt. Loss	Fiber % Wt. Loss	Fiber % Wt. Loss - Control % Wt. Loss
Control	800 - 825	1	.25	33	10	0
		3	.25	52	33	0
Bi_2O_3 added	800 - 825	1	.38	34	11	1
		3	.29	48	30	-3
Pb_3O_4 added	800 - 825	1	.85	39	14	4
		3	.52	54	39	9
Control	700 - 725	1	.24	33	9	0
		3	.26	51	33	0
Bi_2O_3	700 - 725	1	.33	32	10	1
		3	.30	48	30	-3
Pb_3O_4	700 - 725	1	.81	41	17	8
		3	.64	51	40	7
Pb_3O_4 X 10	700 - 725	1.5	8.6	86	81	48

1. SEM Analysis-morphology

Scanning electron microscopy was used to examine oxidative attack enhanced by Pb catalysts. Figure 2 is an SEM micrograph of the virgin AS fiber at 2000X magnification. The striations in the long direction of the fiber result from the PAN fiber processing. These striations are the only distinguishable features on the virgin fiber surface. Figure 3 is a typical micrograph of partially burnt fibers from a Pb_3O_4/Epon 828 composite. The white film in the center and top is probably PbO or Pb_3O_4 left after the epoxy is burnt off. The film in the lowest section of the micrograph is epoxy residue. The morphology of the oxidation attack is highlighted in Figure 4, where a single fiber is displayed at high magnification, 10,000X. The oxidative attack appears to etch craters into the fiber and the craters are not necessarily associated with visible particles. Large particles, in fact, seem inert. Another SEM micrograph, presented in Figure 5, indicates that a different mode of attack also occurs, as evidenced by the transverse lines on the fibers.

In Figures 6a and 6b, SEM micrographs show the AS fiber Pb_3O_4/3501-6 epoxy composite. Unlike the other composites, this sample usually self-extinguished immediately after removal from the oven heat source. Area A appears similar to previous oxidation micrographs with amorphous particles and craters present. Area B, in contrast, contains particles that are crystalline and no signs of oxidative attack are visible.

Fig. 2 — SEM micrograph of virgin as fiber, 2,000x

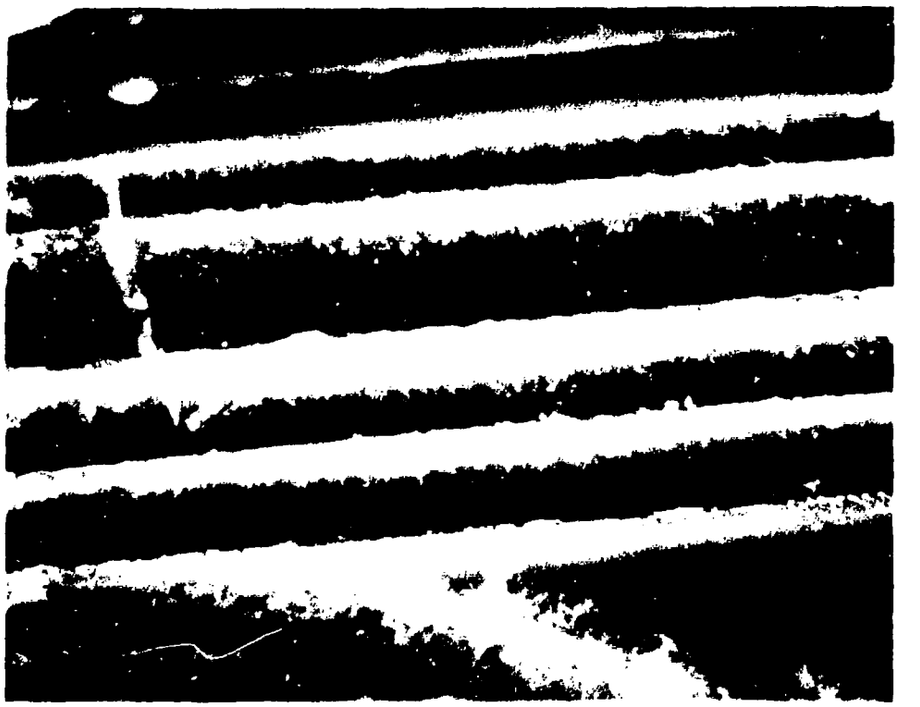

Fig. 3 SEM micrograph of Pb_3O_4-Epon 828 composite as fibers after epoxy burnoff 2,000x

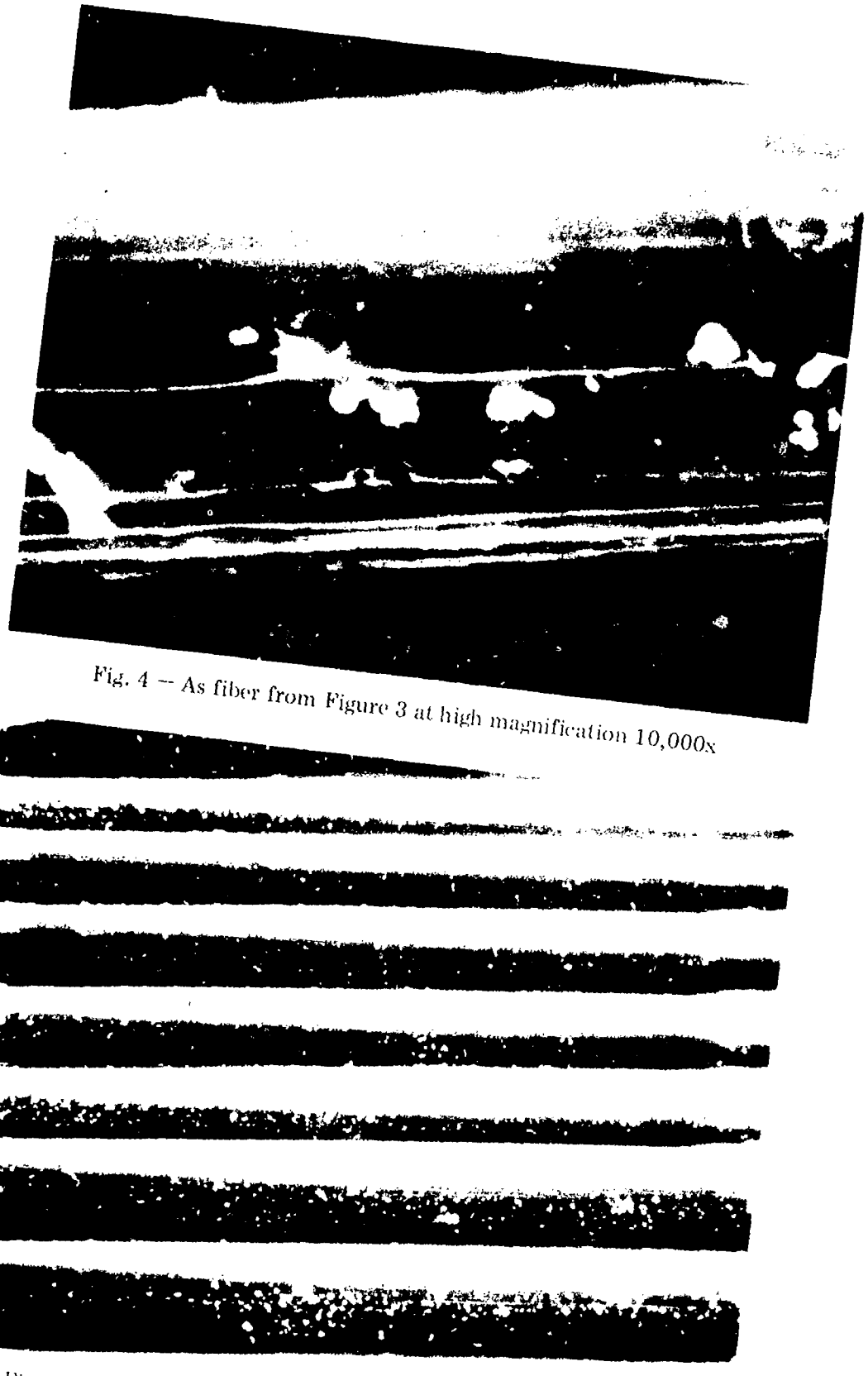

Fig. 4 -- As fiber from Figure 3 at high magnification 10,000x

Fig. 5 -- SEM micrograph of Pb_3O_4-Epon 828 composite T-300 fibers after epoxy burnoff 2,000x

Fig. 6 — SEM of Pb_3O_4-3501-6 composite fibers after epoxy burnoff 2,000x 6a Area A, 6b Area B

Since the morphology of the two areas was so different, we also measured the x-ray emission produced by the electron bombardment in order to determine the elemental composition. The x-ray energies of EDAX spectra are specific to different elements with the proviso that elements of lower atomic number than Na cannot be detected. The only detected element in significant concentration was Pb and the Pb x-ray intensities were proportional to the amount of particles in the analysis area. Representative EDAX spectrum are displayed in Figure 7. This was true of both areas in Figure 6 and the Pb_3O_4-Epon 828 composite. The EDAX spectra did not indicate an elemental difference between the two areas.

A major limitation of the EDAX elemental analysis was its insensitivity to light elements. Ken Clark of NADC, who also noted the inhibiting effect of AS 3501-6 epoxy, hypothesized that it may be due to residue compounds of boron or fluorine which are present in the 3501-6 epoxy. Both elements are known oxidation inhibitors. The Epon 828 epoxy only contains C, H and O, whereas 3501-6 epoxy contains C, H, O, S, and BF_3. In order to determine light element composition, we utilized electron spectroscopy.

2. Electron spectroscopy analysis - surface elemental composition by XPS and AES

X-ray photoelectron spectroscopy relies on x-ray bombardment to eject core level electrons from the surface atoms.

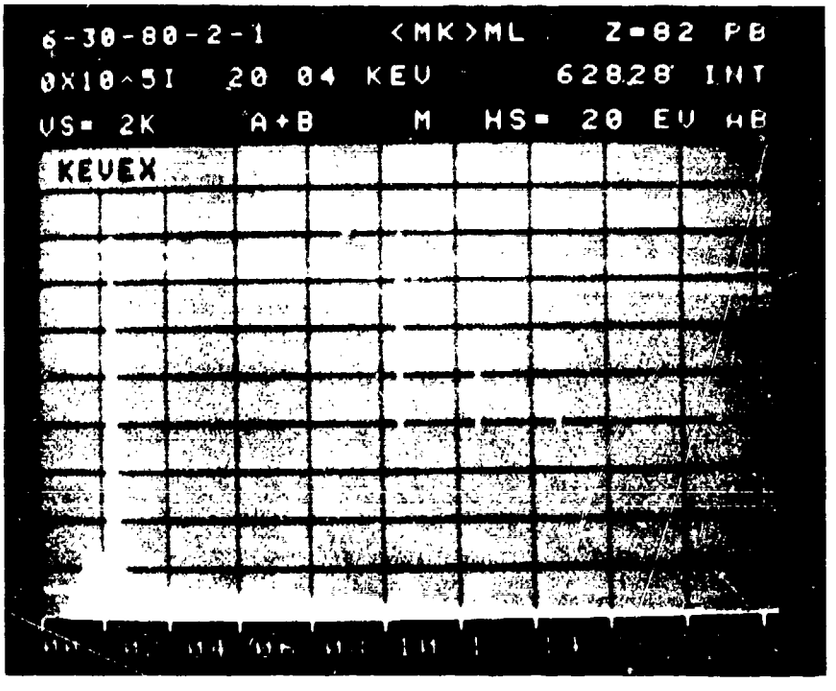

Fig. 7 -- Energy dispersive x-ray analysis (EDAX) spectrum of particles on carbon fibers showing Pb is major constituent with automatic number above 23.

These electrons are collected and energy analyzed by subtracting the measured kinetic energy from the bombarding x-ray energy to determine the electron binding energy. Auger electron spectroscopy (AES) uses electron bombardment to create core holes and then analyzes the Auger electrons which are emitted during dexcitation of the atom. In both cases, the emitted electron energy and intensity can be used to determine the elements present in the sampling volume. Since carbon is easily detected, our results are presented in atomic ratios of impurity elements to the major element carbon in the carbon fibers. The concentrations are only semi-quantitative due to the heterogeneity of the oxidized fiber surfaces and the extreme sensitivity of electron emission to surface depth (96% of the electrons below 50-100 Å are inelastically scattered and never escape the surface). The results are presented in Table 9. XPS was used for Pb, O, C and AES for S, O, N, C, due to the relative analytical technique's elemental sensitivity and reproducibility. Sulfur, oxygen and nitrogen were the major impurities on the fiber surface. Some sodium was also found on the T-300 fiber surfaces. Boron and fluorine were not detected on any of the fiber surfaces. The available AES and XPS instruments did not have sufficient lateral resolution for single particle analysis.

The results show that Pb surface concentration is directly proportional to Pb concentration in water solution when the fiber is solution-dipped and also to Pb_3O_4 concentration in the epoxy when the composite is ignited and the fiber extinguished. The surface oxygen concentration is also quite high for composite

Table 9 — Relative atomic ratios of elements on carbon fiber surface

Sample	Carbon	Oxygen	Nitrogen	Lead	Sulfur
T-300 Fibers dipped in XM $Pb(OAc)_2$ salt in aqueous solution					
.1 M Pb	100	-	x	3.0[1]	-
.05 M Pb	100	-	x	1.6[1]	-
.01 M Pb	100	-	x	.5[1]	-
Composite fiber after epoxy burnoff					
AS, .61g, Pb_3O_4 100 g Epoxy 828	100	4.6[1], 10.[2]	3.6[2]	1.1[1]	<.1[2]
AS, .12g, Pb_3O_4/100g Epoxy 828	100	4.1[1], 1.2[2]	2.9[2]	.2[1]	<.1[2]
AS, .6g PB_3O_4 100g 3501-6	100	22[1], 7.5[2]	2.3[2]	2.3[1]	2.6[2]
Virgin fiber from fabric with finish					
AS	100	.2[2]	2.2[2]	-	<.1[2]
T-300	100	.3[2]	3.1[2]	-	-

[1]XPS measurements

[2]AES measurements

fibers, with the 3501-6 epoxy leaving larger amounts than the Epon 828 at the same Pb_3O_4 epoxy concentration. In terms of oxidative promotion, we note that treatments which leave <1% Pb had a much higher SIT (.01M Pb water solution) and did not sustain combustion (.12 g Pb_3O_4 in Epon 828). However, the Pb concentration on the AS fiber from the 3501-6 epoxy is >1% and the anomaly in the oxidative reactivity is not explained by low Pb concentration.

Both measurements of oxygen intensities confirm the high oxygen surface concentration in the composite fibers. Nitrogen impurity from the PAN fiber precursor was also detected. The only 3501-6 residue element, which was not present in a significant amount from any of the other fiber treatments, was sulfur. Boron and fluorine concentrations were below detection limits, <.1%.

In summary, the microscopy section shows the morphology of oxidative attack. The anomaly of the two areas in 3501-6 AS fibers was not correlated with a difference in elemental composition. The 3501-6 epoxy left a detectable S residue in contrast to the Epon 828. Sulfur is a known oxidative inhibitor and may also have combined with Pb to make the Pb relatively inert; $PbSO_4$ has been reported as the least effective Pb salt (1). Further experimental work would have to be performed in order to clarify the inhibiting effect of 3501-6 epoxy residue.

C. Effect on Oxidation of Experimental Conditions

During the above experimental research it was found that several experimental conditions had an effect on the combustion characteristics. Two of the variables were examined in detail by varying the experimental conditions and measuring the weight loss rate and ignition temperatures.

1. Air Flow and Sample Geometry

The effect of air flow has been previously noted in that low air flows reduced the combustion enhancement by the promoters (3). The relationship between air flow and weight loss was investigated using the Dupont TGA. The weight loss vs. temperature curves were produced at the same heating rates on equivalent samples with different air flows. The results are presented in Table 10. The combustion rate equals the rate of sample weight loss after ignition. In Table 10, the combustion rate follows an $(\text{air flow})^{1/2}$ relationship, as shown by the comparison between the columns $(\text{Airflow/50 ml})^{\frac{1}{2}}$ and the Rate Norm to 50 ml Rate. This relationship has been used to describe a diffusion-controlled reaction where the concentration of the gas reactant at the surface is the controlling factor. The increase in laminar flow velocity reduces the "stagnant" film thickness of product gases at the film surface. The oxygen diffusion rate is determined by its diffusion coefficient and the thickness of the film.

The preceding data were obtained when the samples remained in the heat source. In the self-sustained combustion mode, the percentage of fiber weight loss has also been correlated to air flow (4). At air flows higher than natural convection, it was, invariably, found that composites achieved greater weight loss

Table 10 — The effect of air flow in fiber combustion

Material	Air Flow (ml/min.)	$\sqrt{\frac{\text{Air Flow}}{50\ \text{ml}}}$	Combustion Rate %/min.	Rate Norm to 50 ml rate	SIT (°C)
T-300 6 ply composite control	50	1	6	1	580
	150	1.7	11	1.8	575
T-300 6 ply composite Pb_3O_4	50	1	6	1	500
	150	1.7	11	1.8	485
	250	2.2	18	3	475
		$\sqrt{\frac{\text{Air Flow}}{30\ \text{ml}}}$		Norm to 30 ml	
T-300 tow Pb Acetate solution	250	2.9	24.8	2.1	370
	30 ml	1	11.7	-	-

percentage up to the 90-95% limit. Such promoters as bismuth and copper were found to be effective under these conditions. The 0.1 g atom/100 g Pb_3O_4 treated AS fiber 3501-6 epoxy composite alsc experienced 90-95% wt. loss at higher flow rate conditions.

Another experimental observation was that the normalized weight loss rate of multi-ply composites was approximately inversely proportional to the number of plies in the composite. The slower rate for thick composites is explained by the outside layer reaction depleting the oxygen content in the gas making contact with the inside layers and thereby decreasing the total rate of oxidation. During the combustion, the observer can easily note the outside layers extinguishing first, while the inside layers continue combustion. The total weight loss is actually greater for the slow inside layers due to the heat loss shielding of the outside layers. Total weight percent loss was independent of number of plies after a certain minimum number had been reached.

2. Fuel Fire Heat Source

In order to simulate the reducing environment of an accidental fuel fire, the composite samples were ignited in a methanol fire whose approximate temperature was 700-800°C (measured by a thermocouple placed above the fire in the sample position). Three tests were performed. In Test A, the amount and rate of fiber weight loss were measured within an open dish methanol fire. In Test B, the composite was ignited in a deep dish with very limited

access to air. In Test C, the composite was removed from the fuel fire and the weight loss measured for self-sustained combustion with open access to air.

The open flame data from Test A is presented in Table 11. The T-300/Epon 828 composites with Pb_3O_4, PbO, CuO, and Bi_2O_3 additives showed a high rate of combustion (17%/min.), while the control sample combustion rate was only 1.6%/min. The Pb compounds were also effective in the other composite systems. The surprising result was the 93% fiber weight loss in the Pb_3O_4-treated AS 3501-6 composite. In this system, the reported 6%/min. rate loss describes the weight loss after an initial slow induction period. This high wt. loss rate was not observed when the composite 3501-6 sample remained in the furnace at atmospheric environment and approximately the same temperature.

Test B results, presented in Table 12, show that fiber consumption within an oxygen-starved region of a fuel fire is very slow. One can therefore expect a substantial number of carbon fibers to survive this type of fire intact. Finally, the self-sustained combustion results of Test C in Table 13 confirm the effectiveness of Pb and Bi for the Epon 828 composites. It was also discovered that Pb-treated 3501-6 composites exhibit self-sustained combustion after exposure to the fire for over 2.5 minutes. The time for epoxy burnoff was <1 min. Shorter exposure times resulted in immediate extinguishing upon removal from the fire. Sample duration within the heat source beyond one minute for epoxy burnoff was not important for other fire or oven self-sustained

Table 11 — Open methanol fire combustion samples $\simeq$ 1 inch from top of methanol liquid

(Test A)

Sample	Fiber	Epoxy	Fabric Ply	Total % Wt. Loss	Fiber % Wt. loss	Combustion Time (min.)	Rate % Fiber/min.
PbO	T-300	Epon 828	6	95	93	5.8	17
Pb_3O_4	T-300	Epon 828	6	95	93	6	17
CuO	T-300	Epon 828	6	95	93	6	17
Bi_2OCO_3	T-300	Epon 828	6	95	93	6	17
Bi_2O_3	T-300	Epon 828	6	95	93	9	11
$Ca(OAc)_2$	T-300	Epon 828	6	78	67	13	5
Control	T-300	Epon 828	6	48	22	13.6	1.6
Sb_2O_3	T-300	Epon 828	6	37	5	12	.4
$CaCO_3$	T-300	Epon 828	6	35	3.4	14	.2
Pb_3O_4	As	Epon 828	4	95	93	6.4	15
PbO	As	Epon 828	4	95	93	8.6	11
$CaCO_3$	As	Epon 828	4	56	25	12	2.1
CuO	As	Epon 828	4	34	3	9	.3
Control	As	Epon 828	4	34	0	9	0
Pb_3O_4	As	3501-6	4	95	93	15	6

Table 11 (Cont'd) — Open methanol fire combustion samples ≃ 1 inch from top of methanol liquid

(Test A)

Sample	Fiber	Epoxy	Fabric Ply	Total % Wt. Loss	Fiber % Wt. Loss	Combustion Time (min.)	Rate % Fiber/min.
Control	As	3501-6	4	40	10	23	.4
2" above fire concentration effect							
Pb_3O_4.011	As	3501-6	4	71	57	17	3.4
Pb_3O_4.005	As	3501-6	4	16	-20	epoxy remained	
Pb_3O_4.002	As	3501-6	4	9	-30	epoxy remained	

Table 12 — Closed fuel fire combustion of 6 ply T-300 Epon 828 composites

(Test B)[1]

Sample	Total % Wt. Loss	Fiber % Wt. Loss	Time (min.)	Rate Fiber % Wt. Loss/Min.
Pb_3O_4	56	32	10	3.2
PbO	43	12	10	1.2
CuO	46	6	10	0.6
Control	36	5	10	0.5
$Bi_2O_2CO_3$	33	-5	9	-

[1]Performed in deep dish with limited air accessibility.

Table 13 — Composite self-sustained combustion after removal from a fuel fire ignition

(Test C)

Metal Composite	Fiber Type	Epoxy	Fabric Ply	Min. in Fire	Total Wt. Loss %	Fiber Wt. Loss %	Burn Time Out of Fire (min.)	Rate Fiber %/min.
$Bi_2O_2CO_3$	T-300	Epon 828	6	1.5	96	94	3.9	24
Pb_3O_4	T-300	Epon 828	6	1.5	95	92	4.5	20
$Ca(OAc)_2 \cdot H_2O$*	T-300	Epon 828	6	1.5	69	49	3.6	14
CuO*	T-300	Epon 828	6	1.5	65	45	3.6	12
Control	T-300	Epon 828	6	3	3[illegible]	1	0	0
Control	T-300	Epon 828	[illegible]	2	31	-1	0	0
Control	T-300	Epon 828	6	1	27	-7	0	0
Pb_3O_4 (.610g)	As	Epon 828	4	1.5	97	96	4.2	23
Pb_3O_4 (.305g)	As	Epon 828	4	1.5	97	96	4.8	20
Pb_3O_4 (.122g)	As	Epon 828	4	1.5	89	84	4.1	20
$CaCO_3$	As	Epon 828	4	1.5	42	2	0.4	5
Control	As	Epon 828	4	1.5	33	-3	0	0
CuO	As	Epon 828	4	1.5	29	-4	0.1	0
Pb_3O_4	GY-70	Epon 828	8	1.5	89	82	1.8	46
Control	GY-70	Epon 828	8	1.5	35	0	0	0

Table 13 (Cont'd) — Composite self-sustained combustion after removal from a fuel fire ignition

(Test C)

Metal Composite	Fiber Type	Epoxy	Fabric Ply	Min. in Fire	Total Wt. Loss %	Fiber Wt. Loss %	Burn Time Out of Fire (min.)	Rate Fiber %/min.
Pb_3O_4	As	3501-6	4	2.5	93	90	6.9	13
Pb_3O_4*	As	3501-6	4	1	34	1	0	0
Bi	As	3501-6	4	5	29	-1	0	0
Bi*	As	3501-6	4	1	27	-3	0	0
Control	As	3501-6	4	2	22	-11	0	0
Control*	As	3501-6	4	1	21	-12	0	0

*Not all of sample ignited.

combustion tests. The explanation may be that the reducing fuel fire succeeds in removing any inhibiting residue from the 3501-6 epoxy. Upon residue removal, the oxidation reaction is susceptible to promotion. Thus, the fuel fire environment may remove the 3501-6 residue left in the oven tests and activate the oxidation promoter. It is probable that the severe exposure conditions, which would lead to the most fiber release, would also remove the residue.

D. Mechanical Testing of Composites

Three 4-ply fabric composites were prepared for mechanical testing of the effect of additives on the strength of the composites. The composite preparation is described in Appendix A. In this case, a post-treatment at 400°F for four hours to ensure maximum epoxy cure was also done. The composites consisted of 4-ply AS fabric with 3501-6 epoxy and .01 g atom/100 g epoxy of Pb_3O_4 and Bi_2O_3 in the case of epoxy-treated composites.

The 45° off axis tensile test was performed on sections 5" long by .5" ± .005", cut by a diamond saw. Plastic tabs were glued onto the ends with Eastman 910 and set at room temperature overnight. The tensile test was on an Instron tensile strength test instrument at .05 in/min. The results are presented in Table 14. No significant differences were measured between the control and the powder-treated epoxy composites.

Table 14 — Mechanical testing of composites by 45° off axis tensile test

Sample	Thickness	psi
Pb_3O_4	.083	40,500
Pb_3O_4	.085	43,100
Bi_2O_3	.083	45,400
Bi_2O_3	.082	47,300
Control	.082	43,300
Control	.083	40,700

III. DISCUSSION

A. Comparison with Results of JPL and NADC

Two other laboratories have also carried out research upon the use of metal additives to promote carbon fiber oxidation. The air flow dependence noted by Ken Clark, et al, has been referred to in previous sections (3). He confirmed the effectiveness of Pb and Bi compounds as additives in self-sustained combustion after ignition. Two types of burn tests were employed at NADC, a continuous burn test where the blast burner used a fuel-air mixture and a self-sustained combustion test where the composites were ignited with a reducing fuel flame with a limited oxygen supply. These tests are similar to the fuel fire tests performed at NRL in Section II.C of this report. In the continuous test, composites with Pb and Bi additives burned at a higher rate than other samples; these composites also consistently lost more weight in the second test. The reducing flame test data also confirmed that essentially no fiber weight loss occurred during exposure to a reducing flame environment. The NADC investigation included the use of primer paints with additives, and the results indicate that this treatment also increases fiber weight loss. The NADC SEM micrographs also display the residue left from 3501-6 composites.

The JPL results have been reported to us strictly on an informal basis.(5) In this work, they concentrated on Ca as the additive. They have measured the effect of additives by TGA and differential scanning calorimetry (DSC). The Ca (acetate)$_2$ additive was found to lower the 50% fiber weight loss mark from 570°C to 510-520°C.

Fiber release measurements showed that the Ca additive considerably reduced the amount of fibers released during a fire scenario. They also reported a synergistic effect where the mixture additive of Li and Ca or K and Ca produced more fiber oxidation than straight addition of the effects of lone promoter addition.

Since the above results were presented informally, our critique is conditional. A comparison between our work and JPL's results is difficult owing to the different tests that were performed. However, we would like to emphasize certain points. First, we found $Ca(OAc)_2$ additives less effective than several other additives. Experimental data has been presented in SIT for fibers soaked in metal acetate aqueous solution and self-sustained combustion for fabrics and composites. These results were also obtained by Reardon et al of NRL[3] and Ken Clark of NADC[4]. Second we did not observe a synergistic effect. When mixtures were used in our tests, the additives' performance simulated the effect of the more active catalyst by itself. At this point further discussion and experimental work is necessary before JPL and NRL work can be directly compared.

B. Carbon Combustion Model

The preceding data are a collection of empirical observations without a framework of basic understanding to explain the significance of experimental results. The purpose of the following discussion is to provide this framework by developing a model which describes the heat transfer process at the surface of the carbon fibers during combustion. The model was developed under a complementary ONR-supported program at NRL[9]. The model is based on the thermodynamic law that the heat generated at the carbon surface

by the oxidation reaction must be balanced by the heat loss mechanisms. Similar models have been developed for solid fuel combustion by D. B. Spaulding (6). Heat and mass transfer calculations are, of course, some of the basic pillars of chemical engineering.

The model development is divided into five sections. The heat generation process of carbon oxidation is described first and appropriate Arrhenius equation values are derived from experimental measurements for lead-treated, sodium-treated and virgin fibers. A calculation of convective and radiative heat losses for different carbon fiber structures is presented second. Third, by calculating geometric surface area/wt. for different carbon fiber structures, the heat generation kinetics which were measured in terms of weight are correlated to heat loss which was determined in geometric surface area. The fourth section presents the heat balance model for self-sustained combustion by combining the heat generation and heat loss equations and explains the effect of catalysts and other variables. The last section correlates this model with the experimental observations.

1. Reaction Rate

The kinetics of carbon oxidation have been studied extensively due to the importance of carbon combustion in industry. As in many kinetic problems, the actual mechanisms of carbon oxidation and metal promotion are still unknown. Most studies have concentrated on defining the reaction kinetics in terms of the Arrhenius equation and predicting the temperature dependence of the reaction. In general, these experimentally derived Arrhenius

parameters are limited to the carbon matrix under study and different forms of carbon have generated large variations in the numerical values. The physical significance of the Arrhenius equation is still in doubt for this reaction.

The behavior of the carbon oxidation reaction has been traditionally divided into three temperature zones, defining different sets of reaction kinetics. The kinetics in the low temperature zone 1 are dominated by the chemical rate of the oxygen and carbon reaction. At the very high temperatures of Zone 3, the chemical rate becomes so fast that an oxygen-depleted layer develops at the carbon surface. As a result, the reaction rate is controlled by oxygen diffusion through the product gases of carbon monoxide and carbon dioxide. At intermediate temperatures, the pore infrastructure of most carbons produces local oxygen pressure variations and oxygen diffusion within the pores becomes a critical factor in the kinetics. The general rate equation is:

$$R = K\,[O_2]_{surface}$$

where K equals the chemical rate. The concentration of oxygen at the surface is also dependent on mass transport rates approximated by:

$$R_{diff} = \beta\,([O_2]_{gas} - [O_2]_{surface})$$

where β = diffusion coefficient.

If one accounts for both the oxygen diffusion rate and the carbon/oxygen reaction rate, the equilibrium $[O_2]$ surface concentration is given by:

$$K[O_2]_{surface} = \beta\,([O_2]_{gas} - [O_2]_{surface})$$

and by eliminating $[O_2]_{surface}$

$$R = \frac{K\beta}{K + \beta} \; [O_2]_{gas}$$

In the low-temperature (Zone 1) regime, $K << \beta$, so the chemical rate dominates while the opposite is true at high temperature (Zone 3).

For the purpose of defining the heat generation kinetics, we are interested in describing reaction rate dependence on temperature. In the low temperature Zone 1, this dependence is affected by the chemical reaction kinetics, which can be approximated by the Arrhenius equation defined below:

$$K = Ae^{-E_A/RT}$$

K = reaction rate

A = pre-exponential factor

E_A = activation energy

R = gas constant

T = temperature of carbon surface in °K

The rate units are determined by the units of A, the pre-exponential factor. In this equation, activation energies are associated with different metal catalysts, while A is affected by catalyst coverage. Assuming that Zone 1 kinetics dominate below ignition, we have made rate measurements of weight loss vs temperature with the Dupont TGA instrument. The experimental details are described in a corollary work (9). The results for the three fiber tows are the following:

$$K_{Pb} = 9 \times 10^{4}\ e^{-20\ kcal/RT}$$

$$K_{Na} = 1.9 \times 10^{8}\ e^{-35\ kcal/RT}$$

$$K_{control} = 1.8 \times 10^{8}\ e^{-39\ kcal/RT}$$

The conditions are ambient atmospheric composition and the treated samples were dipped in .1M aqueous solutions. The units of K for these numerical values are calories/cm^2 in order to balance heat generation against heat loss. The calorie conversion is based on the average ΔH of CO and CO_2 production from $C + O_2$, 5 kcals/g carbon. The conversion from measured weight loss rate to surface area units will be discussed in the surface area section. In terms of the heat balance model, the validity of the Arrhenius equation is not too critical. The important number is the temperature at which the rate becomes significant, this is fairly accurately determined by the two fitting parameters. Large errors in either parameter are compensated for by the other parameter when fit to the measured oxidation rate. In our corollary work we discuss the analytical and physical significance of these equations(9).

At some oxidation rate, the rate becomes so high that the concentration of oxygen at the carbon surface goes to zero and the mass transport kinetics of Zone 3 become rate-limiting. In this zone, the temperature dependence of β, the diffusion coefficient, dominates the reaction rate temperature dependence. Since β has

an approximate dependence of $T^{1.7}$, the transition from Zone 1 to Zone 3 is marked by a decrease from the exponential temperature dependence of the chemical rate to the diffusion temperature dependence. This transition can be experimentally observed at low oxygen partial pressures where ignition does not occur and a typical plot from the literature (7) is shown in Figure 8 where ln (reaction rate) is plotted against 1/T for pure carbon oxidation. At atmospheric oxygen pressure, ignition invariably occurs and a steady burning temperature and a diffusion-limited rate is achieved. Since the diffusion process is dependent on the thickness of the "stagnant film" of product gases, the oxidation rate is proportional to the square root of the flow velocity. Our experimentally observed steady burning oxidation rate is 2 ± .5 cals/cm^2 sec under natural convection and ambient room temperature. The carbon surface temperature at this point was measured by an infrared radiometer to be 700-750°C. Carbon oxidation rates of the samples can then be simulated by the three Arrhenius equations up to the diffusion-limited rate.

2. Heat Loss

The first section describes heat generation at the carbon surface; by describing heat loss in this section, we will set up the equations for the heat balance model.

Heat loss from the carbon surface can occur by conduction in the sample, convection to the air, and radiation from the surface. Due to the small sample dimensions, one can ignore sample conduction.

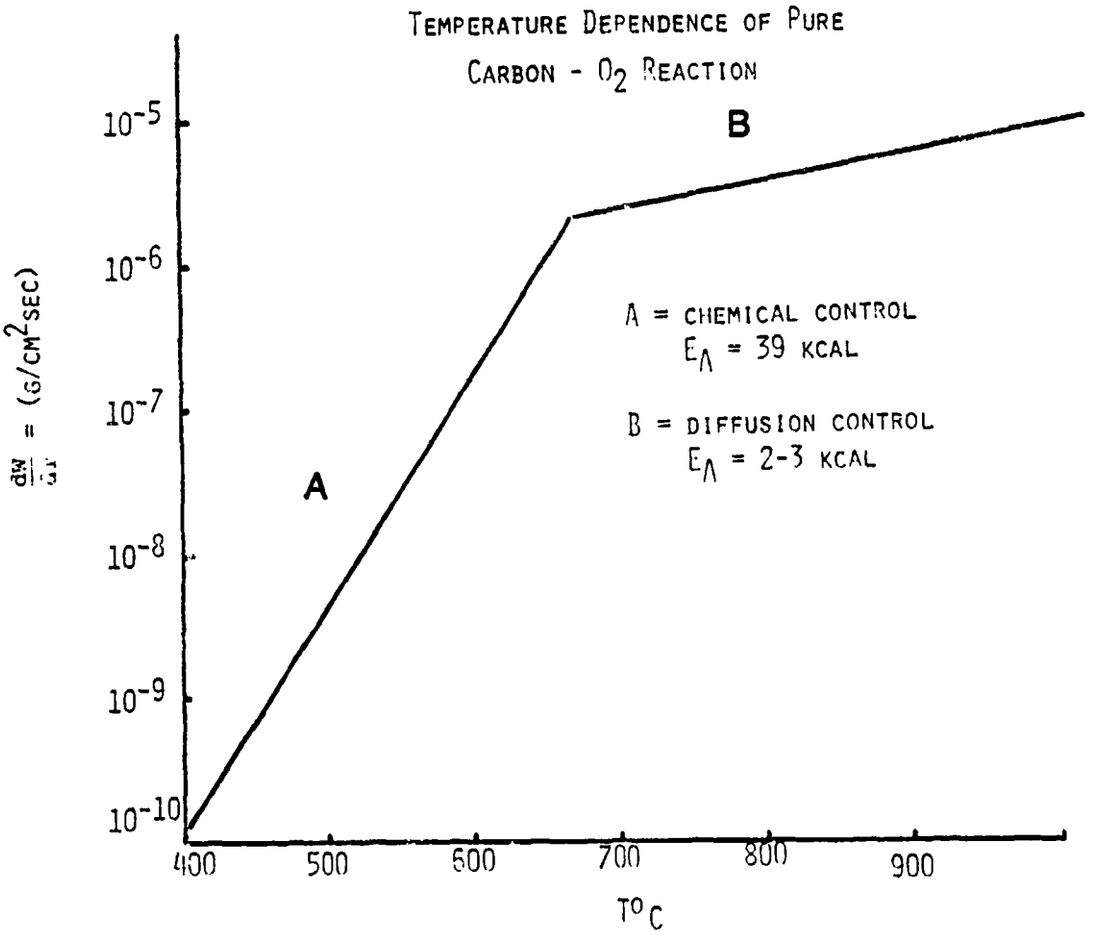

Fig. 8 — Pure carbon-oxygen reaction kinetics dependence on temperature [7]

We will also treat convection as free or natural convection and ignore forced convection which might dominate under higher air flow conditions (i.e., high wind). In general, convective heat loss dominates at low ΔT between the carbon surface and surrounding gas, while radiation heat loss takes over at large ΔT due to its T^4 dependence.

The free convection equation is derived from Brown and Marco's "Introduction to Heat Transfer" (10). Similar treatments are available from most introductory heat transfer treatments. In general, convection heat loss is described by the following equation:

$$Q_{conv} = h_c (T_{surface} - T_{gas})$$

The critical parameter is h_c; the coefficient depends on ΔT between the surface and surrounding gas and the object dimensions. Using the infrared measured temperature of 750°C for burning carbon fiber fabric, the dimensions of tows, fiber and fabric, and approximations when possible, we found single fibers had the largest h_c, 4×10^{-2} cals/cm^{2}sec ^oC while tow h_c was 1×10^{-3} cals/cm$^2{}^oC$. The detailed calculations are presented in Appendix B.

The radiative heat loss calculation is fairly straightforward, being described by the following equation:

$$Q_{rad} = E \sigma (T_{surf}^4 - T_{gas}^4)$$

E = emissivity $\approx$ .9 for black carbon surface

σ = Stefan's constant, -1.36×10^{-12} cal/cm^{2}sec °K

Again, heat loss is given in terms of geometric surface area.

The total heat loss is simply the addition of the linear convective term and the T^4 radiative heat loss.

3. Rate Conversion

Before combining the heat equations into a heat balance model, the oxidation rate must be converted from grams|grams sec to cals|cm^2 sec. This allows direct comparison between heat input and heat loss. In this case, we are only interested in the geometric surface area since this is the critical factor in heat loss. The reaction surface area is probably greater due to surface roughness and some porosity. The actual conversion factor depends on fiber unit (fiber, tow or multi-ply fabric) and the product gas ($O_2+2C\rightarrow 2CO$, ΔH=2.2 kcals|q carbon, $O_2+2C\rightarrow CO_2$, ΔH=7.8 kcal|q carbon). The calorie conversion was made on the basis of a 1 to 1 mixture of CO and CO_2 which is an approximate value (1,6).

The single fiber geometric surface area was calculated using a cylindrical fiber with a diameter of 7-8 μm and a density 1.8 g|cm^3. The resulting conversion factor was 6 x 10^3 cm^2|g. The tow surface area was calculated from a measured diameter of 800 μm (roughly twice the calculated close packed diameter of 3,000 fibers), giving an approximate value of 50 cm^2|g. The single-ply fabric has one-half surface area, 25 cm^2, while multi-ply fabrics are essentially the two outside layers plus the smaller area due to thickness. This leads to an approximate inverse relationship between surface area and number of plies.

The multi-ply and tow conversion factors assumes that reaction only takes place at the outside surfaces. Our experimental observation is that reaction takes place within the inside layers, too. However, outside layer reaction is much faster and the initial

weight normalized reaction rate does follow an inverse relationship with number of plies. A good approximation is that inside layer reaction is significant only after outside layer reaction has extinguished.

4. Heat Balance

In the preceding sections the equations for heat generation by carbon oxidation, heat loss by radiation and convection have been developed. In this section we apply these equations to model the combustion of the carbon surface in order to explain the experimental data.

The experimental sequence for combustion testing was the following: (1) The carbon sample's surface temperature was raised by an external heat source. At each temperature increase the carbon oxidation reaction accelerates, but the additional heat generated is balanced by convective heat loss (dominates at small ΔT between surface and ambient). (2) At the ignition temperature the oxidation reaction accelerates too quickly for heat loss compensation and thermal runaway occurs. The surface temperature is now much hotter than the ambient temperature. At this high temperature the combustion rate is limited by the diffusion rates of oxygen to the surface. The temperature is determined by the heat balance between the heat loss (primarily radiative heat loss at large ΔT) and the heat generated by the reaction. (3) The sample is removed from the heat source so that ambient has dropped to room temperature and the rate of heat loss at the carbon surface is increased. As a result, the combustion temperature drops. At the lower combustion temperature, the oxidation reaction either generates

enough heat to balance the heat loss (self-sustained combustion) or extinguishes. In all stages, the burning rate, carbon surface temperature, and extent of self-sustained combustion are directly dependent on the heat balance at the carbon surface.

The heat balance model for a single tow of T-300 fibers with natural convection and atmospheric conditions is illustrated in Figure 9. The x-axis is the tow surface temperature and the y-axis is the heat generated/lost in cals/cm^2 sec at the carbon surface. The experimental curves K_{Pb}, K_{Na}, and $K_{control}$ represent, respectively, heat generated by Pb catalyzed. Na catalyzed and uncatalyzed carbon oxidation at the surface of the tow (derived) from Section III.1 equations). Curve A represents the total heat loss (convection and radiation) from the tow in room temperature air. Curve C represents the total heat loss into an ambient of 375°C. The heat loss is directly dependent on the difference between the tow surface temperature and the ambient temperature of the surrounding air. The heat generated is only dependent on the carbon oxidation kinetics.

We will now examine the combustion phenomenon using the Pb doped tow as an example. In this initial step, the sample's surface temperature is raised by increasing the ambient temperature Ta. Referring to Figure 9 one follows the process by moving right on the x-axis. For low surface temperature the slope of the heat loss curve is greater than the slope of K_{Pb}. The surface temperature stabilizes at a small ΔT above the ambient and the heat produced by oxidation is too small to be observable in Figure 9. As the temperature increases at some point the slope of $\partial K_{Pb}/\partial T$ becomes

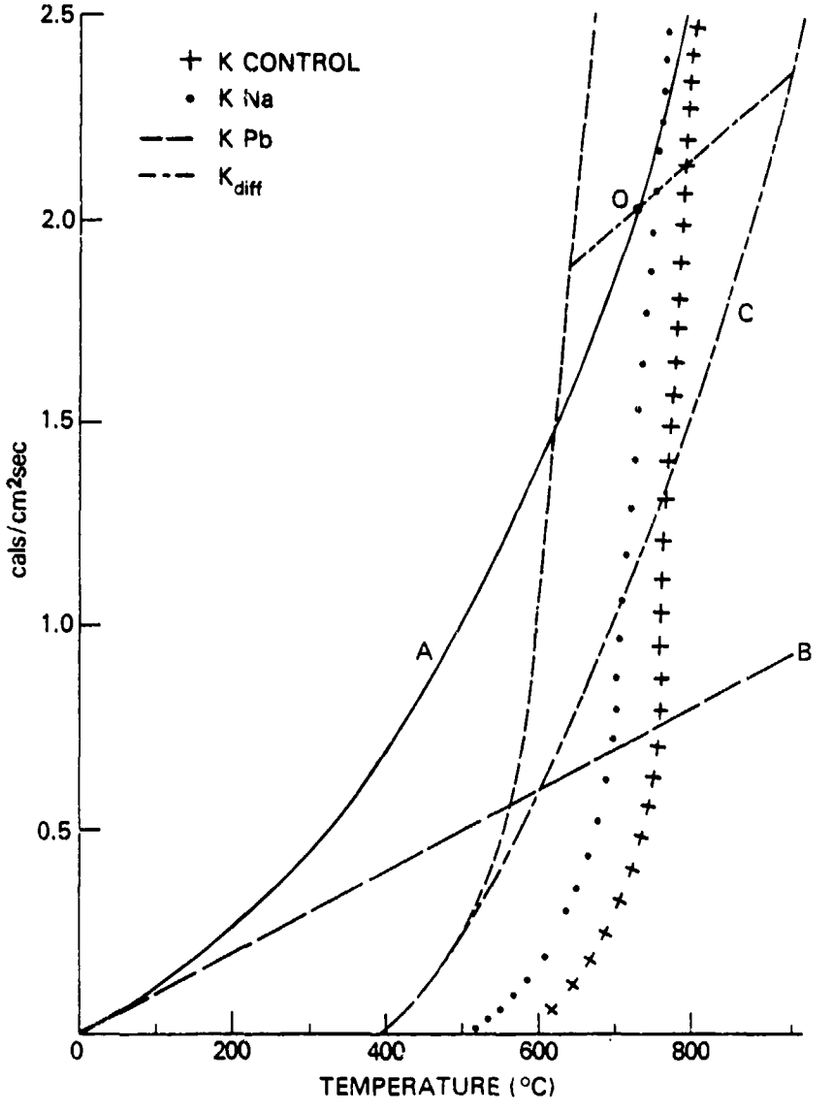

Fig. 9 — Combustion heat balance model for single tow of T-300 carbon fibers

A. Radiative and convective (total) heat loss at room temperature ambient.
B. Convective heat loss at room temperature ambient.
C. Total heat loss at 375°C ambient.
O. Steady burning point of self-sustained combustion at room temperature ambient and natural convection.

greater than the slope of the heat loss curve. This defines the ignition temperature which for Pb doped tows is illustrated in Figure 9. The spontaneous ignition temperatures for Pb, Na and undoped tows are, respectively, 375°C, 475°C, and 550°C. At ignition the exponential dependence of the chemical kinetics increases the generated heat until the oxidation rate becomes dominated by mass transport. The diffusion limited region is shown by the $K_{diffusion}$ line in Figure 9 and has a much reduced temperature dependence. For the ambient T_a = 325°C the steady state burning temperature is very high, described by the intersection of the total heat loss curve with ambient temperature T_a = 375°C and the diffusion limited heat input.

In the last step, the sample is removed from the heat source. The total heat loss is now described by curve A; the heat loss curve has moved substantially to the left. It is apparent that only the Pb catalyzed reaction rate crosses the room temperature heat loss curve prior to the onset of the diffusion limited regime. The Pb catalyzed tows will sustain combustion at the steady state temperature labelled O. The experimentally observed rate of 2 cals/cm^2 sec and temperature of 725°C agree with the point O. The chemical oxidation rates of Na and untreated tows become diffusion limited prior to crossing the heat loss curve into a room temperature ambient and cannot generate sufficient heat to sustain combustion.

This model explains the combustion phenomenon and the effect of metal catalysts upon that phenomenon. The critical factor for

self-sustained combustion is that the chemical rate of heat generation must cross the room temperature heat loss curve before mass transport kinetics limit the oxidation reaction temperature dependence.

Figure 9 was limited to a heat balance model of single tows at ambient room temperature and natural convection conditions. In the experimental sections, we have observed other factors which affect burning parameters. This section explains these effects in terms of the heat balance model.

Ambient temperature: Ambient temperature is the zero point for the heat loss curve. As it is raised, the steady burning point, which is the intersection of heat loss and diffusion oxidation rate, will be raised in temperature. This allows less effective catalysts to sustain combustion.

Sample geometry: Heat generation and radiative heat loss calibrated per unit geometric surface area are not affected by sample size. However, convective heat loss (normalized to cm^2) increases considerably with reduction of sample size. This is shown by fiber convective heat loss/cm^2 geometric surface area being 40 X greater than tow loss. The increase in convective heat loss means that the Pb-catalyzed oxidation rate will never sustain combustion of single fibers under room temperature and convection conditions. The decrease in convective heat loss with size probably accounts for higher weight loss for single-ply fabrics than tows since the heat loss curve is shifted. Multi-ply fabrics have a large decrease in heat loss due to radiative absorption by surrounding layers.

Air flow velocity: Laminar flow velocity increases the diffusion control rate by (velocity)$^{1/2}$ since it reduces the stagnant film thickness by the same power. It also increases convective heat loss by (velocity)$^{0.8}$ (10). Under natural convection conditions, convection heat loss is a small percentage of total heat loss. Therefore, initial increase of flow velocity results in higher burning temperature conditions which enable lower chemical oxidation rates to sustain combustion. This was observed by Ken Clark at NADC (4). As convective heat loss becomes a greater proportion of total heat loss, its higher power dependence on velocity takes over and leads to lower temperatures for sustained combustion, causing reaction shut-off.

Combustion time: As combustion proceeds, the oxidation rate decreases and the heat loss increases. As a result, one usually observes a certain wt. loss combustion cut-off. The wt. loss value depends on the initial reaction rate excess over the required rate-heat loss intersection. Thus, Pb-treated tows only continue to 50% wt. loss, while multi-ply fabrics continue to 95% wt. loss because of the different initial rate-heat loss intersection due to the lower radiative heat loss of the multi-ply fabrics.

IV. CONCLUSIONS

The literature record, our experimental results, and model work have led us to make several conclusions about carbon fiber combustion. First, gasification of carbon fibers at temperatures below 1000°C will only occur through fiber oxidation by oxygen. Other available gas reactants in the atmosphere or fuel fire environments have negligible reaction rates at these temperatures.

This means that the gasification rate is proportional to the accessibility of oxygen. By using the term accessibility, we wish to include all the factors that influence oxygen contact with the carbon surface, such as oxygen partial pressure in the surrounding gas, the flow rate of the ambient gas which influences the oxygen concentration gradient at the carbon surface, and the diffusion coefficient of oxygen within the depleted oxygen film at the surface. This accessibility is a very important variable within the reducing fuel fire heat source, as is shown by the difference in oxidation rates between the "open" and "closed" methanol fires. As discussed in the oxidation kinetic section, accessibility is the only factor influencing the carbon fire oxidation rate at diffusion-controlled temperatures. We have verified this experimentally where fiber oxidation rates inside an oven above 700°C are the same for metal catalysts treated and virgin fibers.

At temperatures below the diffusion-controlled rate, reaction catalysts can increase the oxidation rate considerably. The most effective catalysts are lead compounds. When these compounds are added in sufficient quantity to carbon fibers, they achieve the same oxidation rate as pure carbon oxidation at lower temperature. As a result, lead-treated carbon fibers have an ignition temperature of 375°C rather than 550°C and the transition from chemical to diffusion control will occur at about 625°C rather than 800°C. The ignition temperatures have been experimentally determined and the chemical - diffusion transition temperatures are inferred from the combustion model diagram.

As we have tried to illustrate in the combustion model diagram, the catalyst-induced sustained combustion depends on

the heat balance between the oxidation reaction and heat loss. The most dramatic self-sustained combustion differences are achieved when the room temperature heat loss curve is crossed by the catalyzed oxidation curve below the diffusion-controlled regime, and the oxidation rate of the untreated carbon fibers crosses the heat loss curve above the diffusion controlled regime.

Since the oxidation kinetics and heat balance model are dependent on several variables whose values may fluctuate greatly in an accidental fire/explosion, it is difficult to quantitatively predict the effect of metal additives on fiber relase without direct experimental evidence. However, we can make several qualitative predictions within the context of the different scenarios simulated by the fiber release studies (11-17).

In general, oxidation of fibers which occurs at temperatures below 800°C will be greatly enhanced by metal additives, of which Pb compounds are the most effective. In terms of fuel fire scenarios, we postulate that Pb additives will enhance oxidation even though the average fire temperature is above 800°C. This is due to the fact that oxygen accessibility at the carbon surface is always associated with lower local temperatures in the fire since oxygen presence is due to local drafts from fire turbulence. This postulation is bolstered by the methanol fire results where Pb additives increased the oxidation rate in both the "open" and "closed" 800°C fires.

Upon removal from the fire, the extent of self-sustained combustion is dependent on the heat balance parameters. We have found that Pb in the form of oxides at .01 atom/100 g epoxy will

produce 95% fiber weight loss in multi-ply composites transferred to an atmospheric environment immediately after the high temperature exposure. This weight loss is contrasted with less than 10% weight loss by untreated samples under the same conditions. Therefore we feel that in fuel fire scenarios the amount of gasification will be much greater with lead-treated composites.

Some carbon fiber release studies have reported that considerable fiber oxidation takes place in fuel fire simulations and may limit the amount of carbon fiber release. Pb additives or even other less-effective catalysts will increase the amount of oxidation. These additives will also enhance oxidation under more severe heat loss conditions. This may be critical in thin composites when heat loss is larger and relatively high amounts of fiber release have been reported (13).

There are several conditions in which the catalyst additives will not be effective in increasing fiber gasification. Released single fibers have such a high convective heat loss that combustion will extinguish immediately upon removal from the heat source. Release under blast velocity conditions may also extinguish combustion due to the convective heat loss coefficient at high velocities. Finally, the fiber oxidation reaction depends on accessibility of the oxygen reactant and removal of the epoxy residues from the carbon surface.

In conclusion, metal additives may be quite effective in burn scenarios where fiber release occurs gradually from epoxy-free composite fabric. They will not affect single fibers after release by either burn or burn/blast scenarios.

REFERENCES

1. P. L. Walker, Jr., M. Shelef and R. A. Anderson, Chemistry and Physics of Carbon, Vol. 4, 1968, pp. 287-385.
2. Metal Ion Catalyzed Combustion of Carbon Fibers and Resin Matrices, J. Reardon and L. Russell, 14th Carbon Conference, Pennsylvania State University, June 25-29, 1979.
3. J. Reardon, S. Kaufman, and L. Johnson, Combustion Promoters for Safe Disposal of Carbon Fiber Reinforced Plastics, NRL.
4. K. Clark, Catalytic Incineration of Graphite Fibers in a Graphite/Epoxy Composite Fire, NADC Technical Report NADC-80079-60, May 20, 1980.
5. Novel Approaches for Alleviation of Electrical Hazards of Graphite-Fiber Composites, K. Ramaholli, Jet Propulsion Laboratory Publication 79-63, 1979.
6. "Some Fundamentals of Combustion," D. B. Spalding, Academic Press, Inc., 1955.
7. E. A. Gulbranson, K. F. Andrew and F. A. Brassert, J. Electrochem. Soc., Vol. 110, No. 6, 1963, p. 476.
8. G. Bleyholder and H. Eyring, J. Phys. Chem., Vol. 63, 1959, p. 1004.
9. Interim report for Office of Naval Research, J. Ganjei and J. Murday, to be published.
10. "Introduction to Heat Transfer," A. I. Brown and S. M. Marco, McGraw-Hill Book, Inc., 1958.
11. Burn/Blast Testing of Thornel 300 Composites, MSWC TR 79-78, April, 1980.

12. Assessment of Carbon Fiber Electrical Effects, NASA Conference Publication 2119, Langley Research Center, Hampton, Va., Dec. 4-5, 1979.

13. Potential Release of Fibers from Burning Carbon Composites, NASA TM 80214, July 1980.

14. Burn/Blast Tests of Aircraft Structural Elements, NSWC/DL TR-3897, December 1978.

15. Fiber Release from Impacted Graphite Reinforced Epoxy Composites, NSWC TR 80-216, June 1980.

16. Burn/Blast Tests of Miscellaneous Graphite Composite Parts, NSWC TR 79-390, November 1979.

17. Have Name Conference at NSWC, Silver Spring, Md., June 1980.

APPENDIX A

Preparation of Composites

System 1 - Union Carbide T-300 Fiber with Epon 828 Epoxy and Versamide 125 Curing Agent

For T-300 composites containing six plies of T-300 fabric, 5-7/8" x 5-7/8" square and weighing 25-26 grams, 22 grams of resin were required. The resin was prepared by weighing 13.2 grams of Epon 828 and 8.8 grams of Versamide 125 in separate pools on an aluminum plate. The metallic element which was expected to promote the combustion of the composite materials was weighed separately as an oxide or a salt after grinding to a fine powder. The catalyst concentration used was 0.01 g-atoms of metallic element per 100 grams of resin. Immediately prior to applying the resin onto the fabric, the oxidation catalyst was sprinkled on the aluminum plate and the three ingredients were combined by gentle folding with a spatula.

Composite Layup Procedure

Two stainless steel plates (8"x8" and 5-7/8" x 5-7/8") were sprayed with tetrafluoroethylene release agent for easy removal of the finished composites. Two peel-plies, two plies of glass fabric, and another peel ply were successively stacked on the larger plate. The layers of carbon fabric were then centered in a felt dam 6"x6" square. The resin mixture was applied to the top ply of fabric in small quantities and was worked into the layers by pressing with a spatula. Successive additions were applied so that the entire amount of prepared resin/catalyst mixture was evenly distributed. The layup was then completed with the addition of another peel ply and the smaller stainless steel plate.

T-300/Epon 828 Versamide Cure

The composite layup was placed in a Mylar bag between two hot plates and the bag was evacuated with heating to 90°C. While still under vacuum, the temperature was held at 90°C for one hour and was increased to 120°C and held constant for two hours or longer. The heat and vacuum pump were turned off, and the assembly was allowed to cool gradually to room temperature before removing and weighing the composite.

System 2 - Hercules AS Fiber with Epon 828 Epoxy and Versamide 125 Curing Agent

For these composites, four plies of AS fabric 5-7/8"x5-7/8" square, weighing 30-31 grams, were used, and 26.7 grams of resin were required. The resin was prepared using 16.0 grams of Epon 828 and 10.7 grams of Versamide 125. The concentration of the oxidation catalyst was 0.01 g-atoms of metallic element per 100 grams of resin, as before.

The composite layup procedure and cure were identical to those of the T-300 composites.

System 3 - Hercules AS Fiber with 3501-6 Resin

For AS composites containing four plies of AS fabric 5-7/8"x5-7/8" square and weighing 30-31 grams, 20-21 grams of 3501-6 resin were required. The resin was weighed out in a beaker and was dissolved with heating (<80°C) in a minimal amount methyl ethyl ketone(MEK). Once the resin was completely dissolved, the amount of oxidation catalyst required to provide 0.01 g-atoms of metallic element per 100 grams of resin was added, and the composite was assembled as before. The solvent used to dissolve the resin was removed in a vacuum oven under vacuum at 250°F (120°C) for 35 minutes prior to the cure.

After removing the solvent, the vacuum was released and the assembly was held at 250°F (120°C) for an additional 30 minutes. The oven temperature was then increased to 300°F (150°C) for 40 minutes and, finally, to 350°F (175°C) for 70 minutes before the heat was turned off and the assembly was allowed to gradually cool to room temperature.

APPENDIX B

Calculation of Convective Heat Loss*

$Q_{convective} = h_c A (T_{surface} - T_{gas})$

h_c = convective heat loss coefficient

A = area of surface

When surface is surrounded by air:

$h_c = C \frac{k}{L} (a L^3 \Delta t)^d$ Btu/hr ft^2 °F

a = product of Grashof and Prandelt numbers

C = coefficient of geometry

L = length, $\frac{1}{L} = \frac{1}{L_{hor}} + \frac{1}{L_{vert}}$

Δt = difference in temperature between surface and gas

d = power coefficient dependent on $(a L^3 \Delta t)$ when $aL^3\Delta t \leq 10^{-4}$, d = 0, $aL^3\Delta t$ is 10^3-10^9, d = 1/4.

For tow

C = .55 for cylinder

L = .08 cm = .0026 ft

k = .03

Δt = 750°C

a = $:04x10^6/ft^3$ °F

k = .03 Btu/(hr)(ft)(°F)

$aL^3\Delta t$ = 1.12 so d > 0 and < .25

if $aL^3\Delta t < 10^{-4}$, d = 0

$aL^3\Delta t$ is 10^3 - 10^9, d = .25

$> 10^9$, d = .33

10^{-4} - 10^3 d > 0, d < .26.

* Equations derived from Reference 10.

Assume maximum heat loss, d = 0

$\max h_c = .55 \times \frac{.03}{2.6\text{x}10\text{-}3}$

$= 127$ Btu/hr(ft) °F $\times 1.4\text{x}10^{-4}$ conversion factor

$\max h_c = .9\text{x}10^{-3}$ cals/cm^{2}sec °C

approx. $h_c = 1\text{x}10^{-3}$

for fiber, $L = 5.2\text{x}10^{-5}$, $aL^3\Delta t < 10^{-4}$, d = 0

$h_c = .55 \times \frac{.03}{5.2\text{x}10\text{-}5} \times 1.4\text{x}10^{-4}$

$= 4.4\text{x}10^{-2}$ cals/cm^{2}sec °C

for lin^2 fabric

L = .08 ft

d = .25 since $aL^3\Delta t = 3\text{x}10^4$

$h_c = .5 \times \frac{.03}{.08} \times (2.9\text{x}10^4)^{.25} \times 1.4\text{x}10^{-4}$

$= 3.8\text{x}10^{-4}$ cals/cm^{2}sec.